

Geophysical comparison of the three eruptions in the 20th century of Usu volcano, Japan

Izumi Yokoyama¹ and Masaaki Seino²

¹Higashi 1-17-7-1304, Kunitachi, Tokyo 186-0002, Japan

²Shin-hassamu 7-10-9-10, Teine-ku, Sapporo 006-0807, Japan

(Received September 18, 1998; Revised October 9, 1999; Accepted November 26, 1999)

Usu volcano has erupted seven times since 1663. The last three eruptions occurred during the 20th century (1910, 1943 and 1977) and were observed by standard instruments. Although the three eruptions displayed different surface manifestations, they were, similarly, volcanisms derived from dacitic magmas.

In this paper, the three eruptions are compared mainly from the viewpoint of magma movements before and during the eruptions on the basis of geophysical data, i.e. explosive, seismic and thermal activities, ground deformations, and level changes in aquifers. Post-eruption activities are also comparatively reviewed.

Some phenomena related to the three eruptions are reinterpreted: for the 1910 eruption, the cryptodome model of the upheaval is rejected, and the tectonic structure of the craterlet line is proposed; for the 1943 and the 1977 eruptions, the ratios between seismic energy release and deformation are discussed; for the 1977 eruption, a tilt model of the sector deformation is proposed and relationships between anomalous changes in the aquifer level and ground upheavals are discussed.

Magnitudes of the three eruptions are estimated. Tentatively, the 1943 and 1977 eruptions are roughly of the same order of magnitude and the 1910 eruption is one order of magnitude smaller.

1. Introduction

Hokkaido Island, Japan, has been populated since the 17th century and Usu volcano in southern Hokkaido has erupted seven times: 1663, 1769, 1822, 1853, 1910, 1943 and 1977. These eruptions occurred equally in the summit area and at the northern and eastern bases of the volcano with the characteristic features of dacitic volcanism due to the high viscosity of the magma. The eruptions were accompanied by persistent seismic activity, remarkable deformation, including formation of lava domes or cryptodomes, and pyroclastic flows that occurred in 1663, 1769 and 1853.

Its geologic sketch map as of 1977 (simplified from Soya *et al.*, 1981), before the last eruption, is shown in Fig. 1 where the summit crater rim, shown by the contours with hachures, is roughly 450~500 m above sea level (asl). Remarkable lava domes KU (formed in 1663), OU (1853) and SS (1943) are indicated, and the upheaval MS (1910) and undated cryptodomes are shown by broken contours.

In this paper, we name the three eruptions according to their origin years, the 1910, 1943 and 1977 eruptions, respectively. The durations of the earlier two were mainly defined by the surface activity and the last one by seismicity and deformation observed instrumentally. Roughly, their durations were 5, 21, and 54 months, respectively.

The magmas related to the three eruptions are all dacitic, and the differences in their volcanic activity should depend

on the differences in the state of the volcano at the time of each eruption. These include the physical condition of the magmas and vents in the local structure of each eruption site, and the presence of aquifers. These eruptions were observed with successively improved instrumentation during each eruptive period. We refer to detailed descriptions of the eruptions and some quantitative data of seismicity and deformation, including Omori (1911, 1913) and Sato (1913) on the 1910 eruption, and Fukutomi (1946), Minakami *et al.* (1951), and Kizawa (1957, 1958) on the 1943 eruption, and Katsui *et al.* (1978), Niida *et al.* (1980), Okada *et al.* (1981), Yokoyama *et al.* (1981) and Seino (1983) on the 1977 eruption. Furthermore, we have profited from the study of Nemoto *et al.* (1957) in understanding the subsurface structure of the 1943 lava dome.

1.1 Sequences of the three eruptions

The sequences of the three eruptions are briefly described here and the characteristic features of each eruption will be discussed later. Figure 2 is a topographic sketch map showing the major results of the three eruptions as of 1982, after the 1977 eruption.

The 1910 eruption began at the northern foot of the volcano on July 25, after 4 days of precursory earthquakes. The previous eruption was the 1853 summit eruption. The explosions were phreatic ones derived from aquifers, and the ejecta were volcanic blocks and ashes, not juvenile material. The explosions continued for 10 days and were not remarkably violent although nearly 40 craterlets were formed along an arcuate line approximately 3 km long (from K to T in Fig. 2) at the northern foot of the volcano.

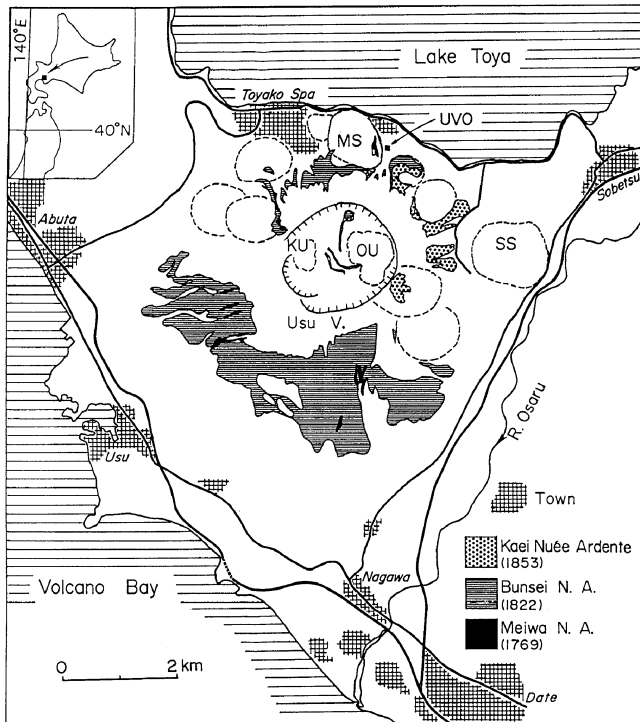


Fig. 1. Geological sketch map of Usu volcano before the 1977 eruption (simplified from Soya *et al.*, 1981). KU: Ko-Usu lava dome (formed in 1663), OU: Oo-Usu lava dome (1853), MS: Meiji-shinzan upheaval (1910), SS: Showa-shinzan lava dome (1943). The others in dashed contours are undated cryptodomes. Contours with hachures show the rim of the summit crater.

The eruption caused an upheaval of approximately 90 m above the original terrace (Meiji-shinzan, MS in Fig. 2), bounded by fault scarps at the southern side. Unfortunately, we do not have sufficient data describing the progress of the eruption due to the sparse population near the eruption sites at that time. Beside piles of volcanic breccia and ashes, upheavals took place more or less around all the craterlets.

The 1943 eruption was preceded by earthquake swarms on December 28, 1943 and the ground upheavals were first observed at Yanagihara village (YH in Fig. 2) at the eastern base of the volcano. The ground had upheaved 23 m over 4 months, and then the activity migrated 2 km north towards Fukaba (FB), where the ground began to upheave, forming a cryptodome by the intrusion of solidifying or solidified magma. Water-assisted explosions (magmatophreatic) first occurred on June 23, nearly 6 months after the occurrence of the precursory earthquakes, and continued until early December 1944 when a spine of solidified lava appeared at the top of the cryptodome (D in Fig. 2). The cryptodome, named the "roof mountain", had attained a height of approximately 170 m and the lava dome (Showa-shinzan, SS dome in Fig. 2) approximately 280 m above the original ground level at the end of 1945.

The 1977 eruption began on August 7, 1977 at the summit and stopped completely in February 1982. It was preceded by 31 hours of precursory earthquake swarms and in the morning of the outburst, a small normal fault was found within the summit crater.

For the first week of the activity, the eruptions were mainly magmatic and four explosion craterlets (Nos. 1~4) were formed in the summit crater. The pumices ejected from the four craterlets are very similar to each other in chemical composition (Katsui *et al.*, 1978). There was no

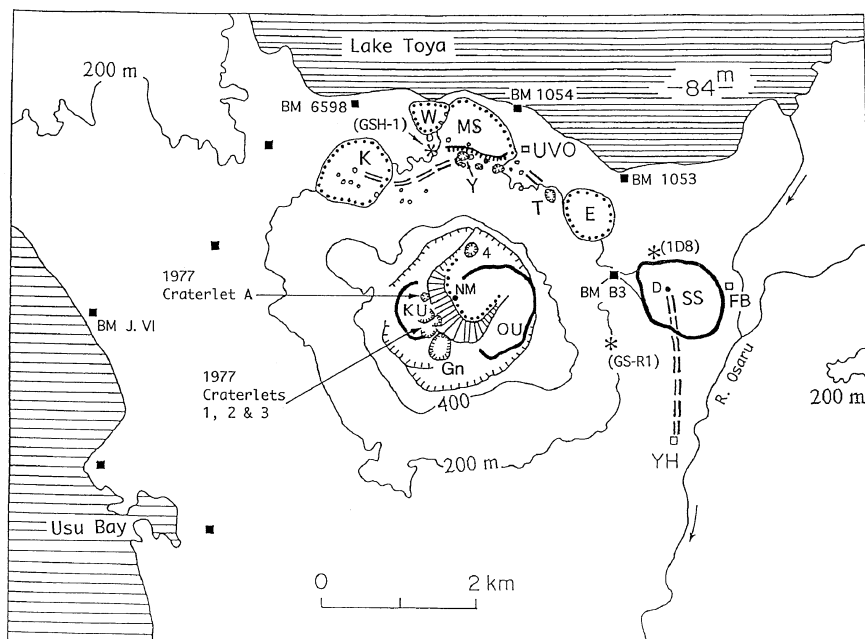


Fig. 2. Map of activity in the three eruptions plotted on a topographic map after the 1977 eruption. Contours with dots show approximate outlines of cryptodomes. MS represents the 1910 upheaval. K and E are not dated. Thick contours show lava domes. SS indicates the 1943 lava dome, Gn the Gin-numa craterlet (1977), NM one of the 1977 peaks. GSH-1, 1D8 and GS-R1 denote the wells. Double broken lines show the lateral extent of volcanic activity.

explosive activity during the following 3 months, but seismicity and ground deformation continued persistently. In November 1977, explosion activity began again, and during the following year, 14 craterlets (A~N) were formed in the summit crater (cf. Fig. 9) by phreatic and magmatophreatic explosions. In August 1978, craterlets J, K, L, and M combined to form the craterlet Gn, where repeated magmatophreatic explosions occurred during the last stage of the surface activities. Craterlet I was very active, especially from April to June 1978, and its fumarolic activity has continued until now, issuing high-temperature gases (cf. Subsection 5.1).

After the craterlet N was formed in October 1978, seismicity and deformation continued at a decreasing level for more than three years. The volcanic activity stopped totally in March 1982. Since the outburst of the 1977 eruption, the summit part had upheaved approximately 185 m, forming the 1977 upheaval or the New Mountain (NM in Fig. 2), and the volcano had thrust first eastward and later northeastward, approximately 200 m in total, forming a U-shaped fault at the center of the summit crater. Its side was approximately 1 km in length.

Pyroclastic flows are known to occur at this volcano. The authors believe the conditions that might cause them were in place during the period of magmatophreatic explosions between June and September 1978, and that the events did not occur by chance.

The three eruptions manifested various explosion types, i.e. phreatic, magmatophreatic and magmatic. Such a classification is not always determinable. In particular cases, the eruption is a sequence of these types, varying with time. For example, the 1943 eruption was of the water-assisted magmatic type (magmatophreatic) for the first 10 days, and later changed to the magmatic type, ejecting much ash, some of which was derived from the new magma during the last stage of the explosion. As another example, the August 1977 explosions were mainly magmatic, but close re-examination indicates the onset of the first explosion was a magmatic steam explosion caused by the rapid vaporization of water contained in magma, and it immediately developed into a magmatic one.

As described above, the three eruptions were all preceded by felt earthquake swarms and their durations ranged from 31 hours to 6 months. Such a wide range may be derived from the variety of magma movements.

1.2 Tectonic settings around the eruption sites revealed by the eruption activities

The subsurface magmas of Usu volcano sought surface vents whether at its summit or at its bases, and the volcanic activities migrated before or during the eruptions. The three eruptions are different from each other in manifestations of volcanic energy which are closely related to the tectonic structures of the eruption sites. Some tectonic settings have been revealed by the eruptions themselves.

The 1910 eruption formed nearly 40 craterlets along an arcuate line at the northern foot of the volcano. The double broken line in Fig. 2 suggests a possible tectonic structure. The 1943 eruption site was located by extrapolation of this tectonic alignment.

The 1943 eruption was preceded by earthquake swarms and ground deformations, both being mutually related. The deformations were upheavals centering at Yanagihara (YH in Fig. 2). We believe that ascending magma remained at a certain depth (approximately 1 km; cf. Section 3) causing the upheaval at YH, and branched out approximately 2 km to the north. Finally, a lava dome (SS) extruded at point D in Fukaba (FB), after three months of explosions there. Such a migration suggests a structural line connecting YH and FB. Explosions could preferentially occur along this line, as well as the alignment formed during the 1910 eruption.

The 1977 eruption started in the summit crater and the magmatic explosions were followed by persistent seismicity and remarkable ground deformation. The deformation of the summit part during the period 1977 to 1982 was determined by repeated measurements of height and distance, and can be generally attributed to tilt movements of the northeastern (NE) sector of the volcano. Figure 3 (top) shows the changes in profile of the volcano in the NE-SW direction, including the 1910 upheaval (MS) and that of 1977 (NM). The NE sector had tilted at an angle of approximately 11 degrees as a block with a hinge located at a depth of approximately 500 m below sea level (bsl) (P in Fig. 3). At the summit, the block is bounded by a U-shaped fault (Fig. 2). The intersection of the block and the fixed ground coincides with the line of the craterlets formed by the 1910 eruption, as previously shown in Figs. 2 and 3. The tilt had resulted in a 185 m upheaval and a 200 m northeastward displacement of the NE sector. In the 1910 eruption, a block at the northern side of the structural line may have tilted causing the MS upheaval (cf. Subsection 2.2).

We know of further evidence of the tectonic line: Fig. 3 (bottom) shows the northeastward displacements of the northeastern slope of the volcano during July 1980 to May 1981 (Maekawa and Watanabe, 1981). This suggests that there are two ground blocks bounded by a discontinuous line of structure that coincides with the craterlet line of the 1910 eruption. The tilts of the NE sector in the 1977 eruption will be discussed in Subsection 4.2.

In short, the three eruptions suggest the existence of a structural line extending at the northern and eastern bases of the volcano.

1.3 Starting depths of the Usu magmas

At present, volcanic activity of Usu volcano is assumed to originate in the magma reservoirs beneath the volcano. In this paper, we are directly concerned with the location of the top of the magma at the start of each volcanic activity. A clue for solving the problem is the hypocentral depths of the volcanic earthquake swarms. We have no accurate hypocentral data for the 1910 eruption even for an earthquake of M 5.5. In the 1943 eruption, according to Minakami *et al.* (1951), the hypocenters of the earthquakes in July 1944 were located at depths of 1.5~5.0 km, though the accuracy was low because determination was based on only four stations. During the period from July 1966 to July 1977, before the 1977 eruption, the JMA (1980) determined the hypocenters of the volcanic earthquakes at depths of 5~6 km. Precursory earthquakes of the 1977

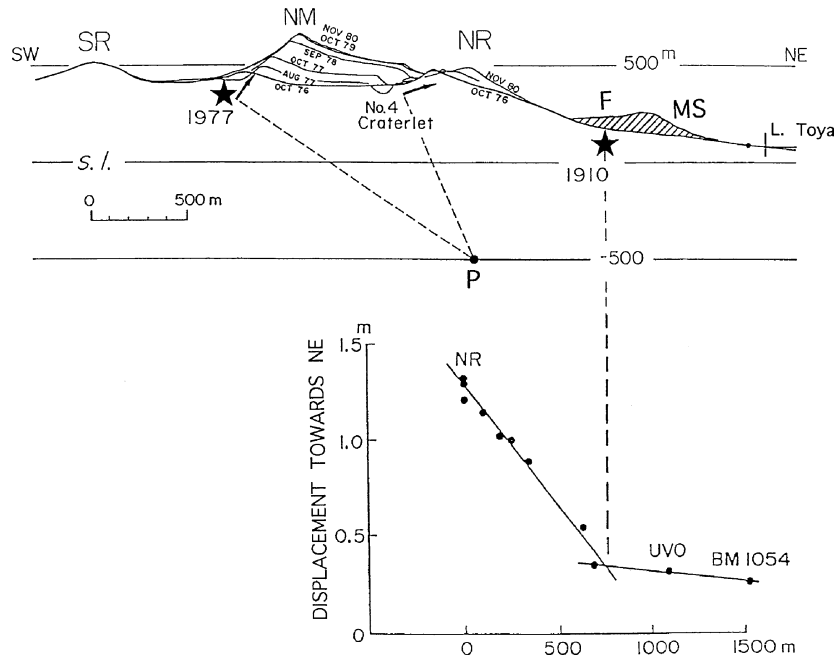


Fig. 3. Tilts of Usu volcano in the 1977 eruption. (Top) Upheavals of point NM at the summit along a SW-NE profile. Star symbols show the craterlets of the 1910 and 1977 eruptions. MS indicates the 1910 upheaval, SR the south rim, and NR the north rim. (Bottom) Northeastward displacements of the northern slope of Usu volcano referring to the UVO during the period July 1980 to May 1981 (Maekawa and Watanabe, 1981).

eruption continued for 31 hours. Suzuki *et al.* (1980) made a temporary observation of these earthquakes at 6 seismic stations for 6 hours and located their hypocenters at depths of 0~5.5 km bsl. After the outburst of the eruption, the earthquakes were all of low frequency and occurred at depths shallower than 2 km. In January 1995, an earthquake swarm occurred beneath the volcano and their hypocenters were determined by the UVO at depths of 4~5 km with high accuracy (Hm. Okada, personal communication). Here, we tentatively assume that magmas should be located at a depth of 5 km immediately before the outbursts of the three eruptions of Usu volcano. This assumption should necessarily lead to the conclusion that magma had ascended from deeper reservoirs or conduits to a depth of 5 km fluidly, unaccompanied by perceptible earthquakes. If the starting depth of the magma was deeper, we would expect faster ascending magmas or more fluid magmas before the outbursts. In this paper, only magma movements that ascended from a depth of 5 km will be discussed.

1.4 Probable depths of magma tops deduced from spatial extents of surface activities

We consider the geometrical relations between the extent of volcanic activities and the depths of their origins, assuming that at these depths, magmas branch forth to form craterlets at the surface: volcanic activities take place at the ground surface fractured by pressure from the magma tops at these depths. For the sake of simplicity, a vertical point-push source is assumed as the origin of magmatic forces. Such a model is known in the discussion of cone-sheet formations by Anderson (1936) who used cases of a semi-infinite medium in three dimensions and gave the possible position of cone-sheets. In Fig. 9 of his

paper, the outermost one intersects the surface at a horizontal radial distance roughly equal to the depth of the source. Thus, the spatial extent of the surface activities depends on the depths of the magma tops. In the cases of the Usu eruptions, an arcuate structural plane pre-exists at the eruption zones. As a rough approximation, we may take the intersections of cone-sheets and the vertical structural plane as magma paths.

1.5 The ratios of seismic energy to deformation, H and η

It is empirically known that deformations caused by dacitic magma movements are accompanied by volcanic earthquake swarms and, especially at Usu volcano, the rates of seismic energy release are proportional to those of volcanogenic deformation (Yokoyama *et al.*, 1981). Deformations may be estimated by volume or height changes. In the Usu eruptions, we adopt upheavals of grounds or extruded lava domes. The ratios are equivalent to the seismic energy released by the achievement of a unit of deformation, in erg/cm. The ratios are classified into one that is associated with extruded lava domes (denoted by H) and another that is related to the ground surface pushed up by intruded magmas (denoted by η). Both ratios are roughly constant at each stage of activity, depending on the deformation mechanisms and properties of the surrounding media. At Usu volcano, we can estimate H for the SS lava dome of the 1943 eruption and η for the 1977 upheaval NM. The seismic energy releases in both eruptions are estimated by seismological data acquired at the Sapporo JMA station.

Upheavals of the SS lava dome were observed by using a transit at a distance of 2.5 km from the dome after May 1945 (Fukutomi, 1946), and its upheaval rate was 0.5 m/

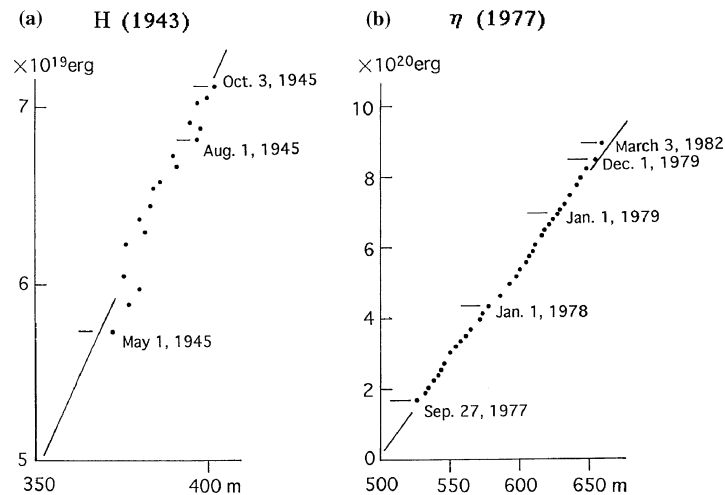


Fig. 4. Ratios of seismic energy release to deformation. (a) 1943 eruption (SS lava dome). The maximum height 407 m was achieved in October 1945 (data after Fukutomi, 1946). (b) 1977 eruption (NM upheaval). The upheaval stopped in March 1982 at a height of 663.28 m (cf. Fig. 14).

day at maximum. The data before May 1945 were obtained by sketches from the same point, and were less reliable. The relation is shown in Fig. 4(a) where the ratio H is estimated at $(4.24 \pm 0.03) \times 10^{15}$ ergs/cm.

On the other hand, the upheavals of the 1977 peak NM were observed by a theodolite and an electromagnetic distancemeter (Yokoyama *et al.*, 1981), and its upheaval rate was 1 m/day at maximum. The relation is shown in Fig. 4(b), and the ratio η is estimated at $(5.33 \pm 0.02) \times 10^{16}$ ergs/cm. It is reasonable that the η value is one order larger than the H value because the ascending subsurface magma body may encounter more resistance than that of the already extruded lava dome. Figure 4 also indicates the upheaval rates in both eruptions.

In the following, we present a detailed discussion on particular subjects for the respective eruptions.

2. The 1910 Eruption

2.1 The magma movements and their contacts with aquifers in the 1910 eruption

The eruption is illustrated in Fig. 5(a) as it relates to the temporal changes of earthquake activity, explosion activity at an arbitrary scale, surface deformation (MS upheaval), and probable movements of magma. Routine seismological data were obtained at the Sapporo weather station (the present Japan Meteorological Agency, JMA), situated at approximately 70 km distance from the volcano. Figure 5(b) shows schematic magma movements at depths shallower than 5 km. The aquifer depths inferred from the well GSH-1 are also shown in the figures. Both figures indicate short-term activity and, in the longer term, earthquakes larger than M 3 occurred during August, September and December, seven times in total, and two small explosions took place in September and October 1910. For the first week of the activity, many earthquakes were felt, including one of M 5.5. Magma pressure increased causing earthquakes and many fissures occurred at the northern base of the volcano. It is noticeable that earthquakes were more frequent in the precursory stage than during the explosions.

After the outburst of the eruption, Omori (1911) began a temporary seismometric observation with his tromometers (4 sec. in proper period). This is the first mobile and successful seismological observation during volcanic eruptions in the world. He remarked that the predominant periods of volcanic earthquakes and tremors, both accompanied by explosions, were 0.5~1.0 sec. and concluded that both had the same properties and origins.

More than 40 craterlets of various sizes exploded in random order along the arcuate line, and all the craterlets were short-lived. These suggest that all craterlets were more or less directly connected to the magma body that was deep down and far below the aquifers, and the magma pressure was not sufficiently high or uniformly distributed to cause activity at all the craterlets simultaneously. Pressure releases through the fissures induced an exsolution of magmatic steam that rushed into aquifer causing phreatic eruptions. Projectiles reached 700 m high at maximum. Some photos of the explosions taken by Omori (1911) show "spear-head" clouds which are a sign of reactions of magmas with aquifers. The ejecta from all the craterlets were fragments of somma lavas and ashes, but no juvenile material. Five craterlets emitted mud flows. It was reported (Omori, 1911) that the terrace at the northern side of the Y craterlet upheaved nearly 90 m for 3 months, forming the MS upheaval (Fig. 2). The averaged rate of the upheaval 1 m/day is rather large and is probably erroneous because only aneroid barometers were used for the height measurements, and also the original topography was not accurately known.

The deformations around the 1910 craterlets were not observed geodetically and we have no quantitative data for the formation of the MS upheaval. The craterlets were distributed along an arcuate line approximately 3 km long. According to Subsection 1.4, the top of the magma body probably ascended to a depth of about 1.5 km beneath the craterlet line (centered near the craterlet Y in Fig. 2), far below the aquifers, the bottom of which was probably 100 m bsl (Fig. 5(a)). At a depth of about 1.5 km, the magma branched into many routes towards the

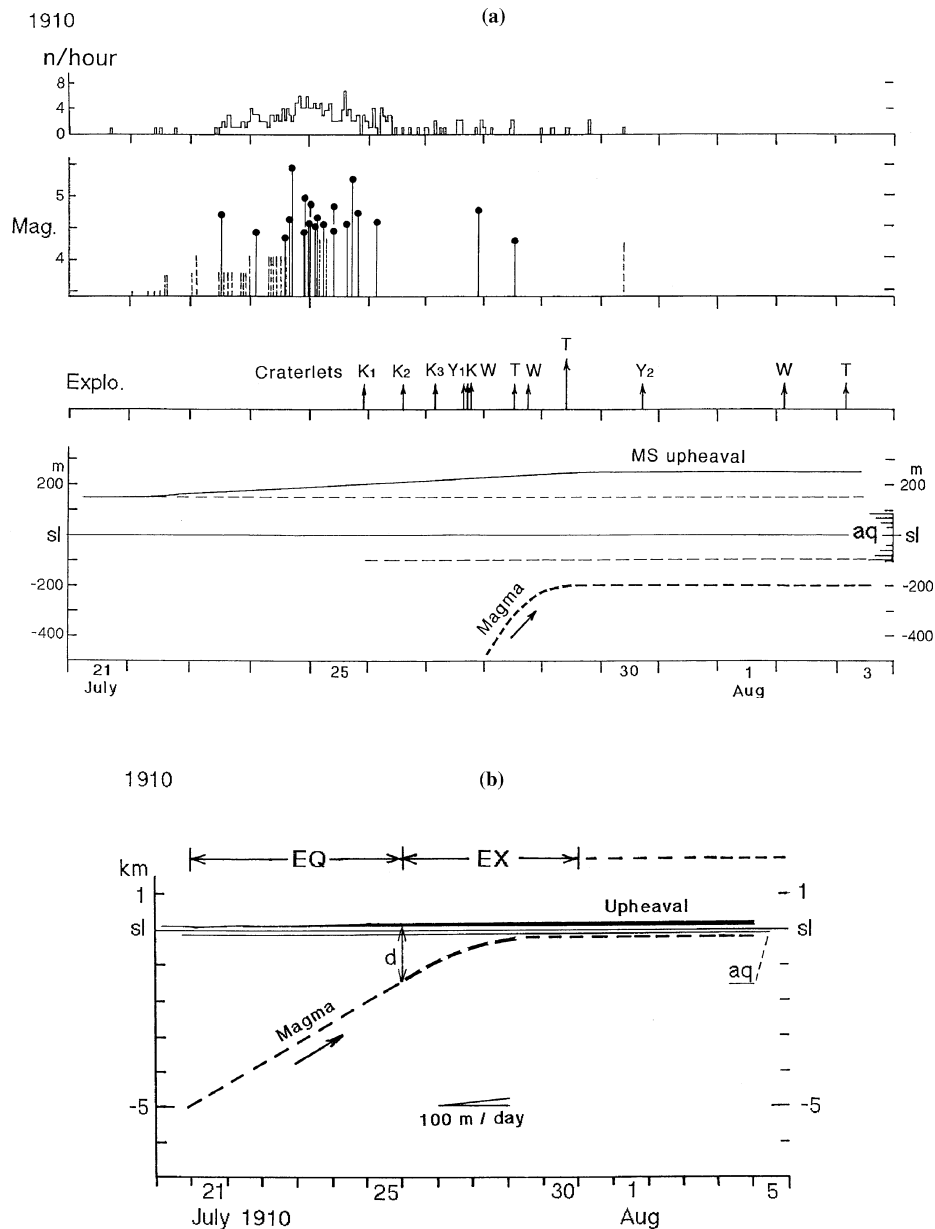


Fig. 5. Temporal changes in volcanic activity of the 1910 eruption. (a) From the top, hourly numbers of earthquakes ($M \geq 3$) observed at Sapporo, magnitude of the earthquakes (broken bars indicate uncertainty of the data), explosivity in arbitrary scale with craterlet notations (K, W, Y and T), upheaval of the MS peak, with an aquifer profile, and a hypothetical process of magma ascent. (b) Schematic diagram of magma movements. EQ: Precursory earthquakes, EX: Explosions, aq: Aquifer (cf. Fig. 10), d: Depth of magma top (1.5 km) deduced from the spatial extent of activities.

craterlets. It is not physically feasible to contain shallow magma bodies that extend over 3 km in length from K to T. Furthermore, the energy supply to the craterlets was not always uniform. Actually, craterlet T at the eastern end of the active zone (Fig. 2) was the most violent and formed the largest depression. A NE-SW profile of the MS upheaval passing through BM 1054 is shown in Fig. 6, where the upheaval is bounded by a fault at the SW side. Sato (1913) mentioned that the lake shore, about 2 km long at the northern side of the MS upheaval, submerged a few meters into the lake and he deduced that both upheaval and subsidence were due to tilting. However, the details of the deformation processes were not clear because they were observed by aneroid barometers, not geodetically and not continuously. There were no craterlets on the top

of the new upheaval, nor on the 1977 upheaval. The craterlets of both eruptions were located beside the newly upheaved parts.

The benchmarks for precise leveling along the roads encircling half of the volcano at its base, were set in 1905. After the 1910 eruption, Omori (1913) found a local upheaval of 2.4 m at BM 6598 (Fig. 2), which was nearest the craterlets. This upheaval was a result of corrugation of the ground caused by the lateral pressure from the eruption sites and the strain exceeded the elastic limit of the crust.

2.2 The origin of the MS upheaval

The MS upheaval has been called a "cryptodome" by Tanakadate (1929): The cryptodome model assumes a shallow magma body to form a domelike upheaval at the ground surface. The MS upheaval is not necessarily

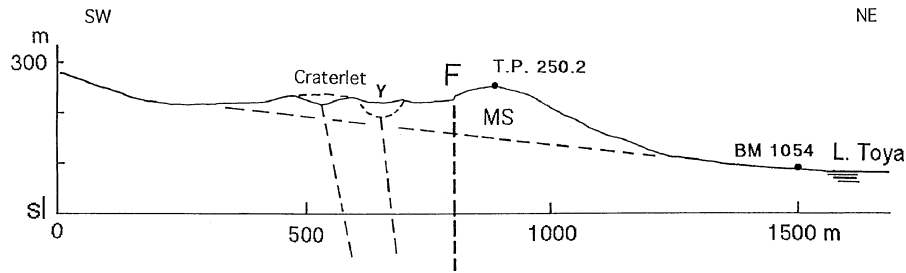


Fig. 6. A topographic section in the SW-NE direction across the 1910 upheaval. Triangulation point 250.2 and BM 1054 were set after 1953. The broken line passing BM 1054 is only for reference. MS: the 1910 upheaval, F: Structural boundary, Y: Craterlet.

domelike compared to the adjacent cryptodomes, K and E in Fig. 2. Evidence for shallow-seated magma in the zone is not always definitive in geomagnetic and gravity anomalies: Nishida and Miyajima (1984) did not find any particular anomalies in the total geomagnetic force on the MS upheaval, and Yokoyama *et al.* (1973) did not find any particular gravity anomalies there, but an approximately 1 mgal higher Bouguer anomaly on the craterlets at the southern base of the upheaval.

The 1910 upheavals were formed alongside the new craterlets. Similarly, the 1977 craterlets occurred beside the new upheaval (NM) as shown in Fig. 9(a). These upheavals were not formed by explosions but by latent magmatic force and underwent tilt movements. In contrast, the 1943 lava dome extruded from the middle of the explosion craterlets.

We have seismological evidence that the MS upheaval is not a cryptodome. Okada (1983) made a comparative study of the earthquake swarms associated with major volcanic eruptions, in which he emphasized that the doming earthquakes of the 1943 and 1977 eruptions were characterized by the nonlog-linear relation between magnitude and frequency in variation to Gutenberg and Richter's (log-linear) relation. In contrast, volcanic earthquakes of the 1910 eruption were characterized by the normal Gutenberg-Richter relation, and the b value of the relation was determined as 0.8 by Okada (1983). This b value is normal for A-type volcanic earthquakes (cf. Subsection 3.1).

Furthermore, by analogy of the 1977 eruption (cf. Subsection 4.2), we suspect that the MS upheaval was formed by thrusting and tilting of the ground, and not by intrusion of shallow magma. In the 1910 eruption, a smaller scale of tilt than for the 1977 eruption was caused by upward pressure exerted by subsurface magma. The magma was not located near the surface because the explosions were not so violent as the other two eruptions, and the main explosions subsided in only 10 days, as shown in Fig. 5. This idea is also supported by the fact that no high-temperature fumaroles were left after the 1910 eruption.

The seismic energy released during the 1910 eruption is known but the related deformations were not known in any detail. The total seismic energy released by earthquakes larger than M 3 is estimated at 3.3×10^{20} ergs. If we adopt the value of η determined for subsurface magma movements in Subsection 1.5, we get the total upheaval as

$$3.3 \times 10^{20} \text{ ergs} / 5.3 \times 10^{16} \text{ ergs/cm} = 62 \text{ m.} \quad (1)$$

As mentioned in the previous subsection, the MS hill reported to have upheaved 90 m may be erroneous. The above estimation may be within a probable range. As the case may be, the tilting of the MS block may have increased its height. After the 1910 eruption, hot springs were found around some craterlets: some of the magma remaining adjacent to the aquifers may supply heat to them.

In short, the 1910 eruption is characterized by phreatic explosions, i.e. the magma remained below the aquifers without making contact with them. Rather, magmatic gases rushed into the aquifers causing phreatic explosions. The explosion activity declined rapidly one week after the outburst (Fig. 5(a)) when the magma energy had been exhausted. In this case, we do not have sufficient data to draw detailed diagrams of magma movement, but show a rough sketch in Fig. 5(b) where we assume that the 1910 magma started from a depth of 5 km, as discussed in Subsection 1.3, and the magma top was located around 1.5 km bsl, as discussed above. The actual period of precursory earthquakes may be longer than 5 days because the data include only felt shocks. It is concluded that the magma ascended fast, 3.5 km/5 days, approximately 700 m/day at maximum. This means that the magma was fluid there and/or openings of the vents accelerated the magma ascent. For reference, Yokoyama (1997) concluded that the Sakurajima magma (mostly andesitic) ascended at a velocity of 2.0 km/day during the initial stage of its 1914 eruption.

3. The 1943 Eruption

3.1 The magma movements and their contacts with aquifers in the 1943 eruption

The activity of the 1943 eruption is illustrated in Fig. 7 where it can be clearly classified into three stages, i.e. migration of seismic and deformation activities, explosion, and doming. Volcanic earthquakes were first felt at the northwestern foot of Usu volcano at the end of 1943. An earthquake of M 5.0, the largest of the 1943 volcanic earthquakes, took place on January 9, 1944. Kizawa (1958) determined its hypocentral depth at approximately 11 km from observation at 3 stations. In Fig. 7(a), it is noticeable that the seismicity was high at the beginning of the volcanic activity. This is the same as in the 1910 eruption but different from the 1977 eruption.

This eruption was instrumentally observed by Minakami

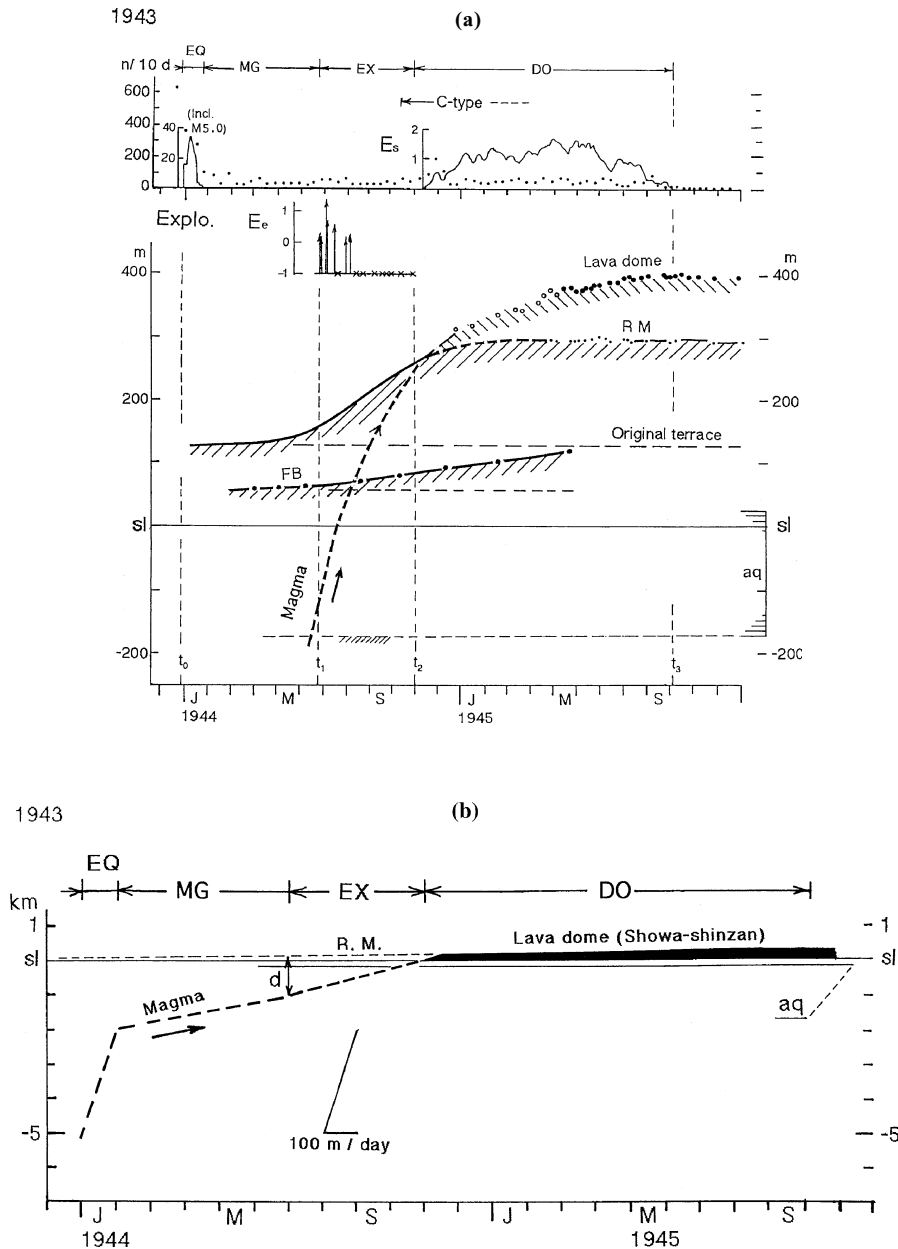


Fig. 7. (a) Temporal changes in volcanic activity of the 1943 eruption. Seismicity in earthquake numbers per 10-day increment (dots), and energy releases (curves) where the units of the energy ordinates are 10^{17} ergs. Explosivity in kinetic explosion energy (E_e), where the unit of the ordinate is 10^{20} ergs (data after Minakami *et al.*, 1951). Magma ascent: Hollow circles indicate visual observations and solid circles instrumental determination. RM: Roof mountain, FB: Fukaba area, aq: Aquifer (cf. Fig. 10). (b) Schematic sequence of magma movements. EQ: Precursory earthquakes, MG: Migration of activity, EX: Explosions, DO: Domeing, d: Depth of magma top, aq: Aquifer.

and his group. Four seismometers registered earthquakes independently, with the timing calibrated by radio time-signals. The Sapporo weather station also registered earthquakes of magnitudes nearly larger than 3. Ground deformations were periodically observed with geodetic methods, and the lava doming was monitored with a transit from a fixed point at a distance of 2.5 km from the dome.

Minakami *et al.* (1951) grouped the earthquakes throughout the 1943 eruption into A- and B-types: The former is similar to tectonic earthquakes, while the latter is of low frequency and has unclear S-phases in wave forms and shallow source locations. This was the first classification according to physical interpretations of

volcanic earthquakes. In addition, they found an earthquake family appeared at the stage of lava dome extrusion and named it the C-type. Its hypocenters were presumed to be at a depth of nearly 0.5 km below the newly forming lava dome. Similar earthquake families were observed at the domeing stage of the 1977 eruption (Okada *et al.*, 1981). Minakami *et al.* (1951) attributed the origin of C-type earthquake families to repetition of the same mechanism for production of the seismic waves at the same location of hypocenters.

Later, Minakami (1960) classified earthquakes of volcanic origin into four types: the A- and B-types of volcanic earthquakes, explosion earthquakes, and volcanic tremors. The classification has been adopted broadly by

volcanologists because of its clearness and of its significance in the volcanic process.

As discussed in Subsection 2.2, the earthquakes in the doming period of the 1943 eruption are characterized by nonlog-linearity in the relation between magnitude and frequency, i.e. magnitude shows a distinct peak against frequency. This means that large earthquakes of a particular magnitude predominantly occur during the period. This magnitude maximum is limited by the dimension of the domeing faults (cf. Subsection 6.1).

Chouet (1996) classified seismic events on volcanoes from wave forms into volcano-tectonic (VT) earthquakes, long-period (LP) events, and tremors. He attributed the origins of VT events to shear failures in the volcanic edifice and those of LP events and tremors to the pressure fluctuations in the fluid. The VT-type corresponds to the A-type and the LP-type is included in Minakami's B-type. Volcanic earthquakes of the B-type observed in the three eruptions of Usu volcano do not have harmonic codas and are different from the LP events. In the three Usu eruptions, contacts of magmas with aquifers controlled the types of explosions but not types of earthquakes.

According to Sawada (1998), the B-type earthquakes of Asama volcano (andesitic), Central Japan, are caused by vesiculation of magmas or separation of gases from magmas in the vents, and the N-type of Asama volcano with harmonic codas, is almost equal to the LP-type of Chouet.

Simultaneously with the earthquake activity, the YH area (Fig. 2) began to upheave and reached its highest level of nearly 23 m. Here, we check the upheaval using the ratio η determined in Subsection 1.5: the energy released by the precursory earthquakes is known to be approximately 4.1×10^{19} ergs. Then, dividing by the value of η , we determine the upheaval as

$$4.1 \times 10^{19} \text{ ergs} / 5.3 \times 10^{16} \text{ ergs/cm} = 7.7 \text{ m.} \quad (2)$$

This estimate is in rough agreement with the observation. The upheaval curves along the route of the precise levels at the YH area were obtained by Minakami *et al.* (1951, figure 24(b)). Assuming a hypothetical point-pressure source for the upheaval, we estimate its depth to be 1.0 km.

Thereafter, the upheaval migrated towards FB, 2 km north of YH. As discussed in Subsection 1.4, the magma top may have been at a depth of about 1.0 km during the migration, far below the aquifer. Hence, we believe that the magma reached that depth causing an upheaval at the YH area and, at first, did not contact the aquifer. The magma then branched towards the north, ascended, and finally contacted the aquifer. The ensuing white smoke was first observed on June 23 (t_1 in Fig. 7(a)), at the point D. Soon after, the magma caused water-assisted explosions for the following 10 days, because the FB area was abundant in water. (Notably, there were fish-hatcheries in that area before 1943.) The explosions rapidly developed into magmatophreatic explosions, ejecting hot mud and ashes. They continued for 4 months ($t_1 \sim t_2$), and four craterlets developed at the roof mountain. The strongest

explosion occurred on July 2. Explosions ended on October 31 (t_2) and, thereafter, much steam issued from the craterlets, and earthquakes occurred continually. Finally, the red-hot lava extruded among the craterlets at the roof mountain in the beginning of December, almost one month after the explosions ended. From this observation, we feel that the magma did not violently react with the aquifer after October 31, probably because its surface had partly solidified and cooled. The roof mountain (RM) and the lava dome (SS) grew up, as shown in Fig. 7(a), partly described from curves constructed by Fukutomi (1946).

The explosion craterlets of the 1943 eruption developed above the magma body, while those of the 1910 and 1977 eruptions were located beside the upheaved zone, as shown in Fig. 2. This indicates that the processes of the 1910 and 1977 upheavals are different from the 1943 lava dome.

The 1943 magma may have extruded, as schematically shown in Fig. 7(b), from a starting depth of 5 km, following the discussion of Subsection 1.3, and the magma top reached a depth of 1 km during the migration period. Then it can be concluded that, during the precursory period in January 1944, the magma was so fluid that it ascended at a velocity of nearly 100 m/day.

4. The 1977 Eruption

The seismic activity and deformation of the 1977 eruption were instrumentally monitored by the Usu Volcano Observatory (UVO) of Hokkaido University and by the JMA. Seismometers were distributed at more than 10 locations on and around the volcano, and almost all the signals were telemetered to the observatory. It is noticeable that the major earthquakes of the three eruptions in the 20th century were recorded by routine observations at the Sapporo JMA station and we can compare all the earthquakes in a uniform way. Deformations were observed by precise levels, a theodolite and electronic distancemeters, and a tiltmeter with signals telemetered and continuously recorded at the observatory. Microgravity, aquifer levels, and SO_2 discharge were measured periodically. Airborne infrared thermographs were taken a few times during the period of eruption.

4.1 The magma movements and their contacts with aquifers in the 1977 eruption

Ground deformations were very remarkable during the 1977 eruption. However, we had no observation of the deformation during the precursory period because the monitoring networks were set up immediately after the outburst. Here, knowing the total seismic energy released by the precursory earthquakes to be 7.1×10^{17} ergs, and using the ratio η determined in Subsection 1.5, we estimate deformation during the precursory period to be

$$7.1 \times 10^{17} \text{ ergs} / 5.3 \times 10^{16} \text{ ergs/cm} = 13 \text{ cm.} \quad (3)$$

This upheaval value is agreeable with the fact that a small normal fault found in the morning of the outburst along the path in the summit crater had a throw of approximately 40 cm. This verifies that precursory earthquakes were accompanied by upheavals as well as those earthquakes of

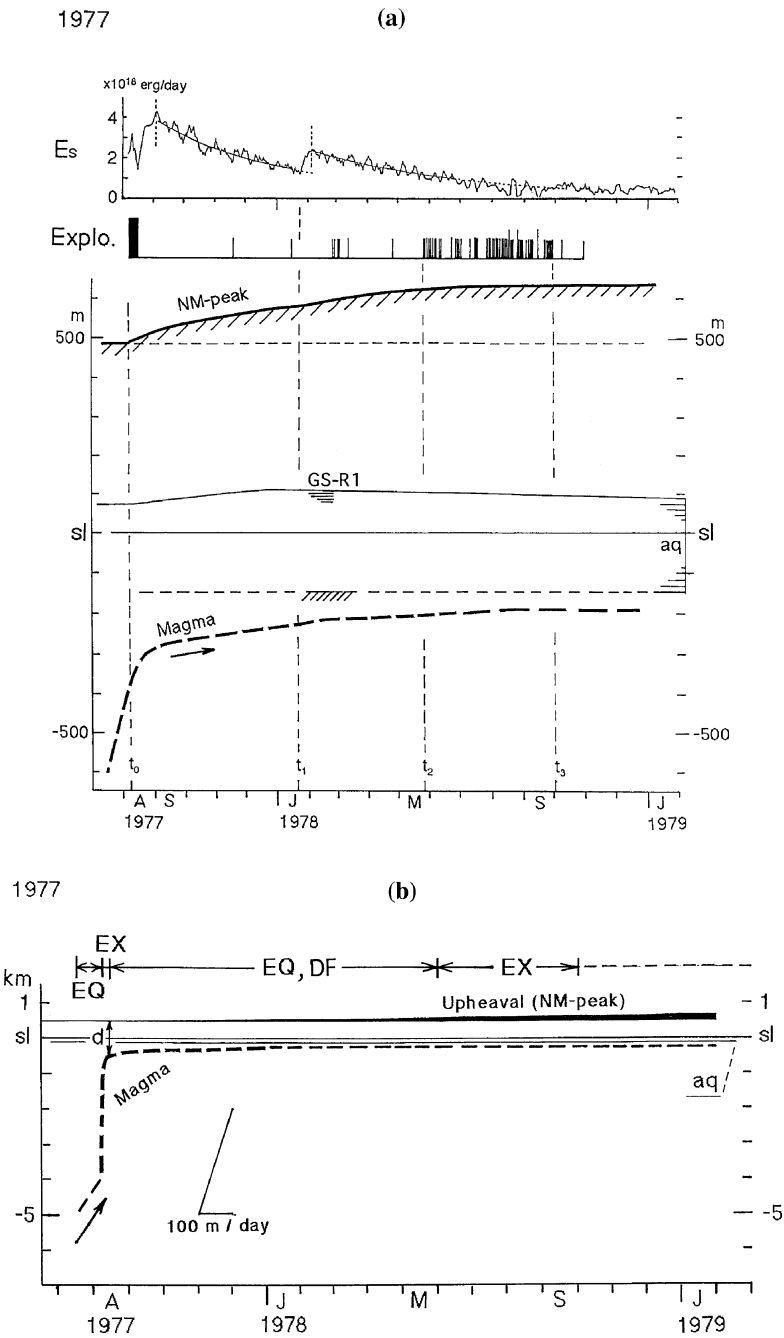


Fig. 8. Temporal changes in volcanic activity of the 1977 eruption. (a) Sequentially from top to bottom: Seismicity in energy releases, explosivity in arbitrary scale, upheavals of the NM peak, and magma ascent. Data of the aquifer (aq) are from the well GS-R1 (cf. Fig. 10). (b) Schematic diagram of magma movements. EQ: Earthquakes, DF: Deformations, EX: Explosions, d: Depth of magma top, aq: Aquifer (cf. Fig. 10).

the succeeding eruption activity.

The 1977 eruption is schematically summarized in Fig. 8. Magmatic explosions of a sub-Plinian type occurred in the first week of the activity. The very first explosion commenced quietly (t_0 in Fig. 8(a)), unaccompanied by any detonations, but soon after explosion clouds gushed to a height of 12 km and formed No. 1 craterlet. In Fig. 8, we suppose that the magma ascended very rapidly and steam exsolved from the magma exploding far below the aquifer, and a vent reached the surface. Then, magmatic steam gushed up, barely contacting the aquifer. The commencement of the first explosion may have been a "magmatic steam explosion" as a forerunner of the

following (dry) magmatic explosions. The No. 2 craterlet exploded the next day. Nos. 1~3 craterlets overlapped, but they had distinctly separate vents, as shown in Fig. 9(a). We may say that the magma system branched out at a shallow depth above the aquifer, judging from spatial extent of the three craterlets (cf. Subsection 1.4), and surfaced at different positions due to the very local structures, as schematically shown in Fig. 9(b). The extent of the craterlets in the 1977 eruption ranged over 1.5 km between the craterlets Gn and No. 4. A point pressure source at a depth of roughly 0.8 km can produce such a lateral extent. In Fig. 9(b), the main vent branched into three, Nos. 1, 2, 3 group, A~N group, and No. 4 at a depth

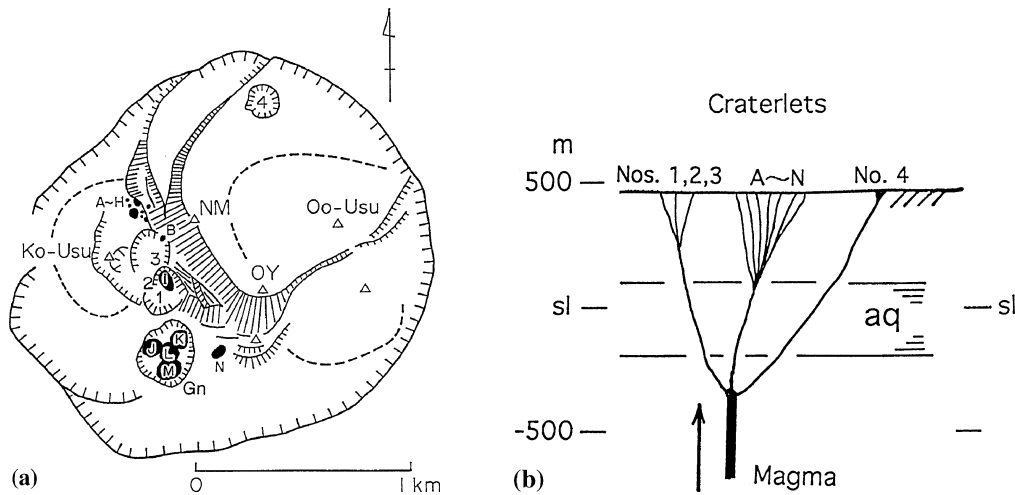


Fig. 9. (a) Distribution of the 1977 craterlets in the summit crater as of 1980. The craterlets J, K, L and M combined into the Gn craterlet in August 1978. (b) Schematic profile of the relative position of the vents of the craterlets, not to scale. Magmas through Nos. 1~4 vents scarcely contacted the aquifer (aq) while those through the A~N vents did so.

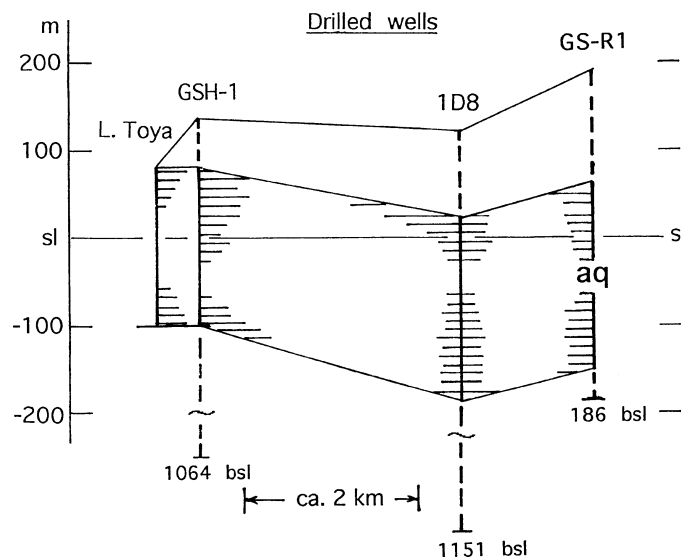


Fig. 10. Schematic profiles of the aquifers (aq) around Usu volcano deduced from the drilled wells (data after the Hokkaido Geol. Surv.).

of approximately 0.8 km below the surface. The magmas of Nos. 1~4 vents scarcely contacted the aquifers, but those of the A~N vents did so from time to time, causing the phreatic and magmatophreatic explosions at these craterlets.

Interactions between magmas and aquifers are important in the discussion of magma behavior. Although we have no wells at the central part of Usu volcano, there are three helpful wells at the northern and eastern bases of the volcano (Fig. 2), GS-R1, GSH-1 and 1D8, drilled in 1966, 1970, and 1982, respectively. Schematic profiles of the wells and the aquifers are shown in Fig. 10 where the aquifer bases are of Neogene Tertiary at a depth of 150~200 m bsl. It may be possible that the aquifer beneath the volcano changed its level with the progress of the activity, as will be discussed in Subsection 4.3. Under certain circumstances, the existence of the volcano may disturb the aquifers in the region. In the discussion of the 1977

eruption which was a central eruption, we extrapolate the aquifers from the periphery to the center, with a rough approximation.

In the first week of the 1977 eruption, four craterlets (Nos. 1~4 in Fig. 9) were formed and each explosion continued for a few hours in total. All four explosions were mainly magmatic and may have been driven by steam pressure derived from the magma beneath the volcano. As mentioned above, to explain the distribution of the new craterlets at the summit, the magma top is expected to have been located at a depth of about 0.8 km during the explosions. Among the first four craterlets, No. 4 craterlet (Photo. 1) was peculiar. This is isolated from the others in the summit crater and coincides with a depression which had existed before the 1977 eruption and may have once been a craterlet. The No. 4 craterlet is approximately 100 m across and of conical depression. First it ejected pumices and ashes to a height of



Photo. 1. No. 4 craterlet in the summit crater (Fig. 2) immediately after its formation (photo. Hokkaido Shimbun Press, August 10, 1977). It was about 100 m across and apparently about 50 m deep. The uppermost white layer is the new ejecta of pumice and ash. The craterlet has been filled with debris. As of 1999, it is flat.

approximately 9 km, and then threw out volcanic blocks and bombs. Aquifers or water-containing rocks may be not directly related to explosions of this type. These may be “dry magmatic explosions”.

After the formation of the four craterlets by magmatic explosions, no explosion occurred for three months, although earthquakes and deformations continued. In November, explosion activity resumed in the form of phreatic explosions. As seen in Fig. 8(a), both seismic activity and deformation renewed in January 1978 (t_1). These may have originated from subsurface magma movements. During this stage of phreatic explosions (November 1977~March 1978), eight craterlets (A~H) were formed on the SW side of the U-shaped fault (Fig. 9(a)). In April 1978, the I craterlet was formed in the middle of craterlets 1, 2 and 3. Its incandescent activity measured 750°C (cf. Subsection 5.1). The ascending magma approached quite close to the aquifers and the magma may have sometimes been in contact with the aquifers, causing water-assisted magmatophreatic explosions from June through September 1978 ($t_2 \sim t_3$).

The subsurface magma may have moved upward, as shown in Fig. 8(b) where the magma top is assumed to have started from a depth of 5 km and reached a depth of 0.8 km at the time of the outburst, as mentioned earlier. Then we are led to conclude that the magma ascended very fast during the explosions of the first week.

According to Suzuki *et al.* (1980), the precursory earthquakes of the 1977 eruption had changed their wave patterns about 5 hours before the outburst: the high-frequency B-type shifted to a low-frequency type. When the magma was fracturing rocks at a depth of a few km, the activity may have been accompanied by earthquakes of high frequency. Subsequently, when the magma began to ascend through the open vents, the earthquake signals may have shifted to low frequency.

4.2 Tilts of the northeastern sector of the volcano caused by the 1977 magma movements

The deformations caused by the 1977 eruption including upheavals of the summit part and the northeastward displacement and corrugations of the ground at the NE foot of the volcano, are roughly interpretable by a tilt model. The model, pertaining to a NE-SW section of the volcano, is schematically shown in Fig. 11. In this figure, during the period from August 1977 to November 1980, the hatched part of the NE sector of the volcano had tilted approximately 11 degrees as a block on a pivot indicated by P. The SW side is bounded by a cluster of craterlets including the Gn craterlet (Figs. 2 and 11) and the NE side by the discontinuous line of structure F (Figs. 4 and 11). As indicated in Fig. 11, the dotted part was pushed up to the pivotal depth at P, where it probably contacted the new magma. As stated in the previous section, either the solidifying or solidified magma may have been located at a depth of approximately 800 m beneath the surface. The plan view of the magma body during this period, measuring approximately 0.8 km in diameter, may be bounded by the vents of the Gn and No. 4 craterlets (Fig. 11). The KU lava dome (Figs. 2 and 11) had subsided approximately 60 m as a block by the end of the 1977 eruption, gravitationally compensating a gap produced by the tilts, while the OU lava dome had elevated approximately 2 m, due to effects of the tilts and earthquake destruction.

As for models of magma intrusion, Ogawa *et al.* (1998) carried out audio-magneto-telluric measurements along a profile crossing the summit crater, and attributed resistive zones beneath the crater to an intruded magma body. They proposed a magma body of approximately 200 m in diameter, with its top at about 300 m asl. We feel there is ambiguity in this interpretation of resistive material: we should first consider the physical and chemical conditions of the magma in situ and the overlying structure with

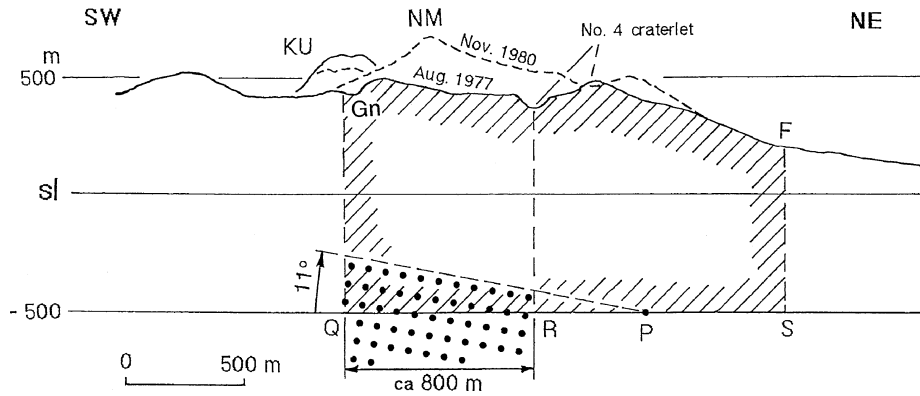


Fig. 11. A schematic tilt model for the deformation due to magma intrusion in the 1977 eruption. Topographic profiles projected in SW-NE direction: Solid line for August 1977; broken line for November 1980. As of 1982, the NM peak had upheaved 185 m and the KU lava dome had subsided 60 m as a block. Shaded part (NE sector) probably tilted 11° , pivoting at the point P. Dotted part probably thrust up the NE sector, causing its tilt. Gn: A combined craterlet, F: Structural line.

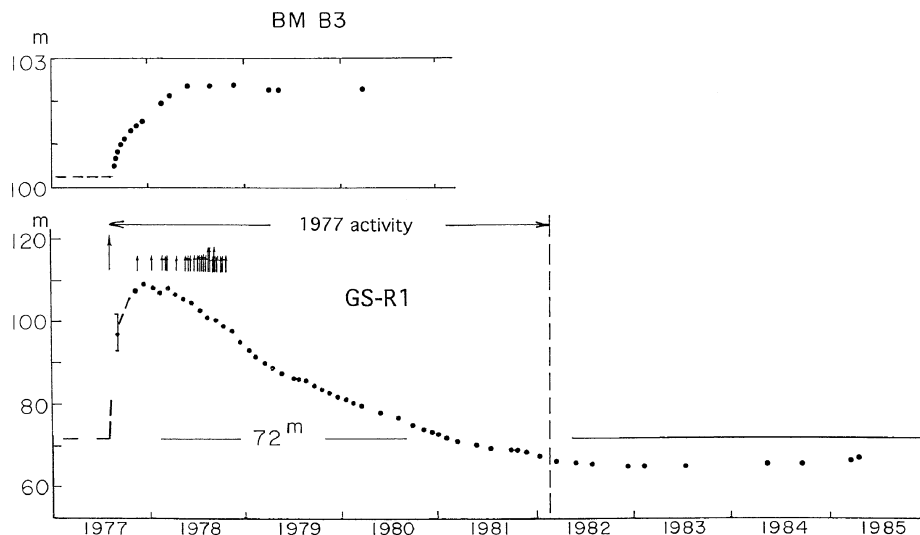


Fig. 12. (Top) Changes in elevation of BM B3 located between the SS lava dome and Usu volcano. The benchmark was demolished due to the construction of a new road after 1980. (Bottom) Changes in water level of the GS-R1 well after July 1977. An error bar is shown for the value of August 1977. Upward arrows indicate explosions in arbitrary scale. 72 m line is the water level of the well before the 1977 eruption.

relation to high resistivity. Furthermore, this model fails to explain the remarkable tilt in the NE sector of the volcano. If magmas intruded to this shallow level, we should observe the corresponding horizontal displacements at the basal part of the volcano (Figs. 3 and 11).

4.3 Changes in the aquifer level at the well GS-R1 accompanied by deformations

The changes in the aquifer level at the GS-R1 well will be discussed in relation to the deformation at the eastern foot (Fig. 2). The well was drilled by the Geological Survey of Japan at approximately 1 km south of the 1943 (or SS) lava dome, to confirm the subsurface structure of the dome. The site is approximately 190 m asl, and the drill reached a depth of 376 m from the surface (Fig. 6). The temperature distribution in the well had been repeatedly measured after 1967 as a part of monitoring volcanic activity. Changes in the water level since the outburst are shown in Fig. 12 (bottom). In the figure, it is clear that the water level had rapidly increased to a

maximum of about 109 m asl on December 12, and later, gradually decreased. At the early stage of the 1943 eruption, similar anomalous changes in the aquifers were noticed by "eyewitnesses": According to Minakami *et al.* (1951), during the precursory earthquakes, the aquifer level decreased remarkably in the upheaving area, while it increased so much as to overflow from wells and fountains in the adjoining areas.

We now focus our attention on the similarity between the changes in the water level and the deformation at the early stage of the 1977 eruption by considering that both were caused through an increase of magma pressure. Figure 12 (top) shows the upheaval of BM B3 at the western foot of the SS lava dome (Fig. 2). It is probable that the deformation began around August 3, i.e. 4 days before the outburst, as mentioned above. This suggests that the water level simultaneously began to increase with the deformation.

Here, we discuss correlations between the rapid increase in the aquifer level and the upheaval of BM B3 during the early stages of the eruption. The benchmark had risen approximately 2.4 m, achieving maximum by April 1978. On the other hand, the aquifer reached the highest level of approximately 40 m in January 1978, as shown in Fig. 12 (bottom). During this period, the ground at the eastern base of Usu volcano was corrugated due to compression by the lateral pressure from the volcano. After that, the benchmark remained at approximately the same height, while the aquifer continued to fall. This suggests that the direction of thrust rotated from the east to the northeast, nearly 45 degrees in the horizontal plane in 5 months, and the GS-R1 well stopped rising earlier than BM B3 did. The time lag was approximately 4.7 months. The strong compression caused deformation exceeding the elastic limits of the uppermost crust, and the ground did not recover to the original state after the compression decreased. On the contrary, the water level of the well dropped gradually with time due to its viscosity and permeability.

5. Post-Eruption Behavior after Each Eruption

Monitoring of post-eruption behavior and analyses of the results are important in studies of volcanic eruptions. They should relate to understanding precursors of the next eruptions. As for the 1977 eruption, post-explosion seismic activity and deformation stopped unexpectedly in February 1982, indicating a total cessation of volcanic activity. Now, secular changes in temperatures of fumaroles, micro deformations of lava domes and volcanogenic upheavals, and aquifer levels will be discussed.

5.1 Secular changes in the temperature of fumaroles

Fumaroles are energized by magmas or their remnants and their temperature is an index of post-eruption activity.

The 1910 eruption formed more than 40 explosion craterlets. According to the observational report by Sato (1913), almost all craterlets were not active and some of them held water at their bottom as of August 1911. The highest temperature of the fumaroles in these craterlets may have been below 100°C, and that of the remnant fumaroles was approximately 60°C as of 1997. This is one of the remarkable contrasts with the other two eruptions; the 1910 eruption was phreatic.

The 1943 lava dome has high temperature fumaroles on its top. The highest temperature was roughly estimated to be nearly 1000°C in 1945, judged from optical pyrometer, and was measured by thermocouples at 980°C in 1947, and 883°C in 1949 (Minakami *et al.*, 1951). Since 1954, the highest temperature at the K fumarole on the dome has been monitored almost periodically. The results are shown in Fig. 13, where the temperature had decreased nearly exponentially with time until about 1980, and later had decreased again exponentially at a different rate. As of 1997, the temperature remained at 190°C. No significant changes were observed in association with the onset of the 1977 eruption, other than some effects on the heat source after 1980. This means that the 1977 magma was not directly connected with the 1943 magma, although the pumices of the 1977 eruptions are very similar in chemical composition to those of the 1943 lava dome. In other words, the 1943 lava dome is a parasitic product of Usu volcano but the geometric relationship is not close.

During the 1977 activity, at the stage of magmatophreatic eruptions, the most active, I craterlet was formed in April 1978. Its temperature has been monitored periodically and was 750°C in 1978, as shown in Fig. 13, and had decreased to approximately 490°C as of 1997.

The high temperature fumarole K on the 1943 dome and at the I craterlet at the base of the 1977 upheaval, have been energized by high-temperature gas flows from the magma remnants beneath the volcano. In Fig. 13, the temperature values of the I fumarole are rather dispersed because, instead of a single vent, it consists of multiple fractures. In the figure, the higher values should be more significant. Both fumaroles K and I took approximately 20 years to cool from 750 to 500°C. This means that heat capacity of both magma masses are roughly equal and their cooling processes are similar.

In contrast, no high temperature fumaroles remained from the 1910 craterlets. This suggests that the 1910 magma was small in total mass and/or deeply located compared to the other two.

5.2 Secular changes in volcanogenic deformations

The 1910 eruption is characterized by phreatic explosions accompanying the formation of new upheavals and nearly 40 craterlets. Their secular changes in height or topography have not been monitored by geodetic methods. The

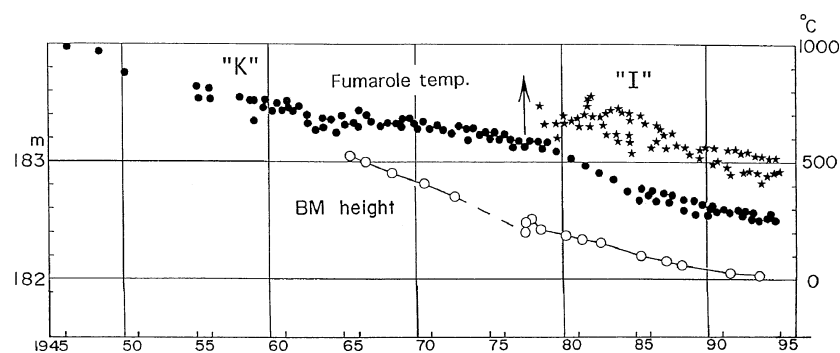


Fig. 13. Secular changes in temperature of "K" fumarole on the 1943 lava dome (solid circles) and "I" fumarole in the 1977 craterlet (star symbols), and those in height of BM B1 on the slope of the lava dome (hollow circles) referring to BM 1053 at the lake shore. The arrow indicates the outburst of the 1977 eruption.

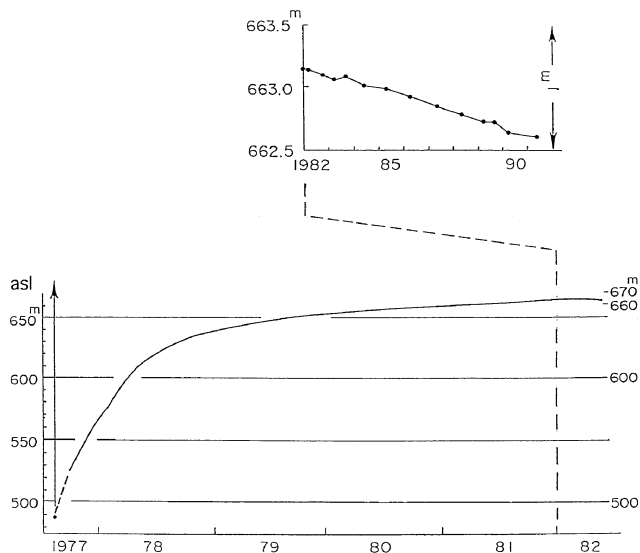


Fig. 14. Secular changes in height of the 1977 NM-peak at the summit crater. In the inset, the ordinate is expanded and the abscissa is compressed.

deformations in the 1943 and 1977 eruptions were observed geodetically with variable completeness. Here, we focus our discussion on the post-eruption behavior of the lava dome of the 1943 eruption (SS in Fig. 2) and the new peak of the 1977 eruption (NM).

The 1943 lava dome became accessible in the 1950s and its height has been monitored by repeated precise levelings since 1965 when five benchmarks were set on the western slope of the dome and its base. Secular changes in height of BM B1, located on the middle slope of the dome, are shown in Fig. 13 where a small disturbance occurred during the early stages of the 1977 eruption. It was due to the eastward thrust from Usu volcano and does not show any direct magmatic relationship between the volcano and its parasitic lava dome.

During the 1977 activity, the NM-peak (Fig. 2) at the summit crater had upheaved approximately 185 m as shown in Fig. 14. It is located at the side of a U-shaped fault. After March 1982 when the seismicity and deformation of the 1977 eruption stopped, the peak began to subside at a low rate, as shown in the inset of Fig. 14. Actually, this was a criterion for the cessation of the 1977 eruption of Usu volcano. Such behavior may be explained by the rheology of the ground material and not by normal thermal contraction of the subsurface magma, because thermal conditions do not change sharply. During the volcanic eruptions, the medium was pushed upward by the ascending magma, and was in an expansional state. After the activity stopped and the upward stress was released, the medium changed to being under the compressional field and began to recover rheologically. An extruded lava dome is also supported by the surrounding medium. The changes in height of the 1943 lava dome (Fig. 13) may be interpreted in the same way, although we have no accurate observations from the end of the eruption.

5.3 Secular changes in water level of the well GS-R1

As already discussed in Subsection 4.3, the changes in

the water level and the temperature of the well GS-R1 located west of the 1943 lava dome, have been observed since 1967. Before the 1977 eruption, we expected some changes in its temperature and, contrary to our expectation, the temperature scarcely changed but the water level drastically changed with the outburst of the eruption, as shown in Fig. 12, and it has not yet settled. After more data are accumulated in the future, a more quantitative interpretation should be expected. In this paper, we emphasize the need to know the structure of the aquifers beneath the volcano more accurately to be able to monitor their changes associated with future volcanic activity.

6. Eruption Magnitudes of the Three Eruptions

The three eruptions with magmas of similar chemical composition have demonstrated various types of volcanic explosions, depending on the relative positions of the magmas to the aquifers and on the respective tectonic circumstances around the eruption sites. In the following, some parameters relating to eruption magnitudes will be discussed.

6.1 Maximum earthquake magnitudes and volcanic activity extent

The maximum magnitude of the earthquakes observed during the three eruptions were 5.5, 4.9, and 4.4, respectively. Here, we check how the activity was when they occurred. In both the 1910 and the 1943 eruptions that were parasitic, they occurred during the precursory or migrating stages where the magmas were seeking surface vents. In the 1977 eruption that was central, an earthquake of M 3.7 took place at the precursory stage, but was not the largest. The largest earthquakes, of M 4.4, occurred repeatedly during the domeing stage and their families formed noticeable nonlog-linear relations (cf. Subsection 2.2). Hence, it seems reasonable to expect that the maximum magnitude of volcanic earthquakes is related to the dimensions of magma movements. Studies of earthquake sources suggest that the size of the fault from which seismic waves are radiated is the most effective factor in influencing earthquake magnitude. In fact, for tectonic earthquakes, Dambara (1966) proposed an empirical relation between the upper bounds of fault length L_m (km) and earthquake magnitudes M (2~8) as $\log L_m = 0.51 M - 2.27$.

The authors attempt to extend this relation to that between the extent of volcanic activity (E_m) and the largest magnitudes (M_m) for the Usu eruptions. The former is determined by the spatial extent of the craterlets or deformations. The relation should be similar to Dambara's formula. Previously, we mentioned the E_m of the three eruptions as 3, 2, and 1.5 km, respectively, and the M_m were 5.5, 4.9, and 4.4, respectively. Though we have only three samples, an empirical formula can be estimated as $\log E_m = 0.30 M_m - 1.2$, where E_m is measured in km. This formula is a little different from Dambara's, as expected.

On the other hand, the total seismic energy released in the 1910 eruption is estimated at 3.3×10^{20} ergs (Okada, 1982), that in the 1943 eruption at 7.1×10^{19} ergs, and that in the 1977 eruption at 9.6×10^{20} ergs (Seino, 1983).

Comparing these three estimates, we may say that the order in magnitude of these values only is significant, and that the movement of the 1943 lava dome was accompanied by relatively small amounts of seismic energy. The total amount of seismic energy may be not an indicator of magma quantity but of resistance against magma movements.

6.2 Energy partition among explosions, earthquakes and deformations;

As reported by Yokoyama *et al.* (1981) and Seino (1983), the three types of energy, explosive, deformation and seismic, are mutually correlated in the 1977 eruption: The three larger explosions in August and September 1978 provide us with the means for estimating the energy partition. After these explosions that hurled incandescent rocks from the Gn craterlet (Fig. 2), the seismic activity of the volcano stopped for a few days to as long as a week. We can estimate the energy of the explosions by knowing their initial velocities and the total mass of ejecta, and the deficiency of seismic energy in the days following the explosion by assuming the normal level of seismic energy releases. The explosion energy should be approximately 10 times larger than the deficiency of the seismic energy. Because the seismic activity parallels the deformation activity, as discussed by Yokoyama *et al.* (1981), it may be expected that the deformation would stop whenever the earthquakes do so. This indicates that the three kinds of energy have a constant amount in total. In fact, both activities were canceled by an explosion and we reach the conclusion that the explosion energy is equal to the sum of the seismic energy and deformation energy. Considering that explosion energy is approximately one order of magnitude larger than seismic energy, we may say that deformation energy is also the same as the explosion energy in order of magnitude.

6.3 Eruption magnitudes of the three eruptions

Magnitudes of volcanic eruptions are not uniquely defined because their manifestations are variable, ranging widely according to the physical properties of magmas. Originally, they should be estimated by masses of magmas directly related to the eruptions, characterized by the quantity of ejecta and various kinds of energy releases. At present, its comprehensive determination is difficult. We may estimate the mass of the ejecta accompanied by energies and the volume of deformations caused by magma movements, and dissipated seismic and explosive energies. Time derivatives of energy releases should be equal to the "intensity" of eruptions.

Considering the above discussion, we prefer to put more weight on the deformation energy than on the seismic energy to estimate magnitude of the eruptions.

The 1910 eruption formed nearly 40 craterlets distributed along an arcuate line approximately 3 km long. Of the three eruptions, this is the longest dimension of volcanic activity and may indicate a greater depth of magma. The maximum earthquake magnitude was M 5.5, but the upheaval was the smallest. The explosions were phreatic and not so explosive, probably because the magma remained deep down. The deformation volume is

approximately $2.0 \times 10^7 \text{ m}^3$, the smallest of the three eruptions.

The 1943 activity migrated approximately 2 km to the eruption site. Only in this eruption did magma extrude, forming a lava dome. The upheaved area and the lava dome extend for approximately 2 km. The deformation volume is approximately $2.3 \times 10^8 \text{ m}^3$, the largest of the three eruptions. The explosivity was the second largest.

The 1977 eruption was the largest in surface deformations, although we cannot exactly estimate the volume of the magma related to this deformation. A side of the U-shaped fault in the summit crater is approximately 1 km long and the horizontal extent of the craterlet distribution is approximately 1.5 km. The deformation volume is estimated at $1.2 \times 10^8 \text{ m}^3$ and the ejecta volume at $0.3 \times 10^8 \text{ m}^3$ in dense rock equivalent and, hence, the total volume, $1.5 \times 10^8 \text{ m}^3$, is roughly the same as that of 1943. The explosivity was the largest because the explosions were magmatic and magmatophreatic at the central crater.

The early explosions of the 1977 eruption were most violent and continued for the longest time compared with the other two eruptions, probably because the former is a central eruption directly connected with magmas, and the latter are parasitic eruptions fed by secondary passages of magmas.

Finally, by preferentially weighing the magnitudes of volcanogenic deformations, we may say that the 1943 and 1977 eruptions are roughly of the same order of magnitude and the 1910 eruption is one order of magnitude smaller.

7. Conclusion

The explosive behavior of the three eruptions can be interpreted by the magma movements relative to the aquifers and tectonic structure around the eruption sites. In this paper, we assume that magmas ascend to a depth of 5 km, judging from the hypocentral depths of precursory earthquakes. One of the problems to resolve in the future is the behavior of the magmas at greater depths.

We suspect that the 1910 upheaval (MS) is not a cryptodome, because the magma top must have remained below the aquifers. The 1943 lava dome extruded after magma passed through the aquifers, causing violent water-assisted explosions. The 1977 magma reacted with the aquifers but did not extrude. The difference in eruption mode among the three eruptions may have originated from varying magmatic pressure and reaction with aquifers.

We reach the conclusion that solidifying dacitic magmas may ascend at a high velocity, a few hundred meters per day, especially when vents are opening. However, when they approach the surface of the earth, they generally slow down and finally stop forming extruded or cryptic lava domes. This means that magma ascents in vents may be caused by lithostatic pressure. In this respect, we need further verification from other volcanoes, i.e. fluid basaltic magmas. Ascending magmas of this type decrease their confining pressure, which leads to exsolution of gases and a rapid increase in volume for accelerated extrusion or fountaining of lava.

A huge tilt movement in the NE sector of the volcano in the 1977 eruption is verified by various observations. The remarkable descent of the KU lava dome in the summit crater may be explained by gravity compensation for a gap produced by the tilt.

It is concluded that the 1943 and 1977 eruptions are roughly of the same order of magnitude and the 1910 eruption is one order of magnitude smaller.

Acknowledgments. The authors owe it to the pioneering geophysicists Profs. F. Omori, T. Minakami and T. Fukutomi that we are able to have access to the valuable data acquired during the 1910 and 1943 eruptions. We are deeply thankful to the staff of the Usu Volcano Observatory (Hm. Okada, Director), Hokkaido University who kindly put their observational data for the 1977 eruption at our disposal. Data on the columnar section of the drillings around Usu volcano was provided by Dr. H. Oshima of Hokkaido University, to whom we are very grateful. We thank Dr. B. A. Chouet whose critical and constructive review improved our early version of the manuscript. We benefited from a discussion on the Usu eruptions with Dr. R. Y. Koyanagi, to whom we wish to express our heartfelt gratitude. Thanks are due to the Hokkaido Shimibun Press that courteously placed Photo. 1 at our disposal.

Reference

- Anderson, E. M., The dynamics of the formation of cone-sheet, ring-dykes, and caldron-subsidence, *Proc. Roy. Soc. Edin.*, **56**, 128–157, 1936.
- Chouet, B. A., Long-period volcanic seismicity: its source and use in eruption forecasting, *Nature*, **380**, 309–316, 1996.
- Dambara, T., Vertical movements of earth's crust in relation to the Matsushiro earthquake. *J. Geod. Soc. Japan*, **12**, 18–45, 1966 (in Japanese).
- Fukutomi, T., On formation of Showa-shinzan, Usu volcano, *Kagaku*, **16**, 3–8, 1946 (in Japanese).
- JMA (Japan Meteorological Agency), The eruption of Usu volcano (August 1977–December 1978), *Tech. Rep. JMA*, **99**, 1–204, 1980 (in Japanese).
- Katsui, Y., Y. Oba, K. Onuma, T. Suzuki, Y. Kondo, T. Watanabe, K. Niida, T. Uda, S. Hagiwara, T. Nagao, J. Nishikawa, M. Yamamoto, Y. Ikeda, H. Katagawa, N. Tsuchiya, M. Shirahase, S. Nemoto, S. Yokoyama, T. Soya, T. Fujita, K. Inaba, and K. Koide, Preliminary report of the 1977 eruption of Usu volcano, *J. Fac. Sci. Hokkaido Univ.*, Ser. IV, **18**, 385–408, 1978.
- Kizawa, T., A study of earthquakes in relation to volcanic activity (I) and (II), *Paper Met. Geophys.*, **8**, 150–169, 1957 and **9**, 204–239, 1958.
- Maekawa, T. and H. Watanabe, Damages caused by ground deformations accompanying the 1977–1978 eruption of Usu volcano, Hokkaido (2nd Report), *Geophys. Bull. Hokkaido Univ.*, **40**, 47–54, 1981 (in Japanese with English summary).
- Minakami, T., Fundamental research for predicting volcanic eruptions (part 1), *Bull. Earthq. Res. Inst.*, **38**, 497–544, 1960.
- Minakami, T., T. Ishikawa, and K. Yagi, The 1944 eruption of volcano Usu in Hokkaido, Japan, *Bull. Volcanol.*, **11**, 45–157, 1951.
- Nemoto, T., M. Hayakawa, K. Takahashi, and S. Oana, Report on the geological, geophysical and geochemical studies of Usu volcano, *Rep. Geol. Surv. Japan*, **170**, 1–149, 1957 (in Japanese with English summary).
- Niida, K., Y. Katsui, T. Suzuki, and Y. Kondo, The 1977–1978 eruption of Usu volcano, *J. Fac. Sci. Hokkaido Univ.*, Ser. IV, **19**, 357–394, 1980.
- Nishida, Y. and E. Miyajima, Subsurface structure of Usu volcano, Japan as revealed by detailed magnetic survey, *J. Volcanol. Geotherm. Res.*, **22**, 271–285, 1984.
- Ogawa, Y., N. Matsushima, H. Oshima, S. Takakura, M. Utsugi, K. Hirano, M. Igarashi, and T. Doi, A resistivity cross-section of Usu volcano, Hokkaido, Japan, by audio-magnetotelluric soundings, *Earth Planets Space*, **50**, 339–346, 1998.
- Okada, Hm., Earthquake swarm activity of Usu volcano in 1910, *Geophys. Bull. Hokkaido Univ.*, **41**, 53–63, 1982 (in Japanese with English abstract).
- Okada, Hm., Comparative study of earthquake swarms associated with major volcanic activities, in *Arc Volcanism: Physics and Tectonics*, edited by D. Shimozuru and I. Yokoyama, pp. 43–61, Terrapub., Tokyo, 1983.
- Okada, Hm., H. Watanabe, H. Yamashita, and I. Yokoyama, Seismological significance of the 1977–1978 eruptions and the magma intrusion process of Usu volcano, Hokkaido, *J. Volcanol. Geotherm. Res.*, **9**, 311–334, 1981.
- Omori, F., The Usu-san eruption and earthquake and elevation phenomena, *Bull. Imp. Earthq. Inv. Com.*, **5**, 1–137, 1911 and 1913.
- Sato, D., Preliminary report on the explosion of Usu Volcano, *Bull. Geol. Surv. Japan*, **22**, 1–46, 1913 (in Japanese).
- Sawada, M., The source mechanism of B-type and explosion earthquakes and the origin of N-type earthquakes observed at Asama Volcano, Central Japan, *Bull. Earthq. Res. Inst.*, **73**, 155–265, 1998.
- Seino, M., Seismic activity accompanying the 1977–1978 eruption of Usu volcano, Japan, *Paper Met. Geophys.*, **54**, 105–141, 1983.
- Soya, T., Y. Katsui, K. Niida, and K. Sakai, Geological map of Usu volcano, 1:25,000, Geol. Surv. Japan, 1981.
- Suzuki, S., H. Yamashita, H. Watanabe, H. Okada, and Y. Nishida, Hypocenters of the premonitory earthquakes to the 1977 eruption of Usu volcano, *Bull. Volcanol. Soc. Japan*, **3**, 181–193, 1980 (in Japanese with English abstract).
- Tanakadate, H. Two types of volcanic dome in Japan, *Proc. 4th Pacific Sci. Congr., Java*, 695–704, 1929.
- Yokoyama, I., An interpretation of the 1914 Sakurajima volcano, *Proc. Japan Acad.*, **73**, Ser. B, 53–58, 1997.
- Yokoyama, I., Y. Katsui, Y. Oba, and Y. Ehara, *Usu Volcano: Its Volcano Geology, History of Eruptions, Present State of Activity and Prevention of Disasters*, 254 pp., Com. Prev. Disas, Hokkaido, Sapporo, 1973 (in Japanese).
- Yokoyama, I., H. Yamashita, H. Watanabe, and Hm. Okada, Geophysical characteristics of dacite volcanism—The 1977–1978 eruption of Usu volcano, *J. Volcanol. Geotherm. Res.*, **9**, 335–358, 1981.